34th Annual International Conference of the IEEE EMBS
San Diego, California USA, 28 August - 1 September, 2012

A Wirelessly Programmable Chip for Multi-channel Neural Stimulation*

Songping Mai, Zhijun Wang, Chun Zhang, and Zhihua Wang, *Member, IEEE*

***Abstract*—This paper presents an implantable inductively powered mix-signal chip for neural stimulation, which is implemented in 0.35-μm high-voltage CMOS process. It features 16 stimulating channels and a maximum stimulating rate of 15Kbps. The frequency, amplitude and width of stimulating pulses are all wirelessly programmable. Charge balance is guaranteed by a flexible switch array at the stimulating output stage. And to reduce power consumption, a dual-voltage-source scheme is adopted also at the stimulating output stage. Measurement results show that the proposed chip consumes less than 1mA at typical working conditions.**

I. Introduction

Electrical stimulators are therapeutically useful for restoring partial functionality to neurologically damaged individuals. It can be applied for instance to victims of spinal cord injuries who have lost control over part of their body (paralysis) or to patients suffering from foot drop [1-6]. And in those well developed medical devices such as pacemakers and cochlear implants, electrical stimulators have also provided a revolutionized treatment for previously incurable conditions.

Several wireless neural stimulators have been described in the literature, e.g. [7-10], each with their distinctive features. Fig. 1 shows a common structure for a wireless electrical stimulating system. Inductive link is employed to power and control the implanted stimulator, since wireless connection is superior to percutaneous wire which provides an infection path into the body. The implanted stimulator recovers both power and data (stimulating instructions) from the wireless signals and drives the electrodes according to the stimulating instructions.

Electrical stimulation will result in oxidation-reduction reaction at the electrode-tissue interface. Therefore, to reduce electrode corrosion or cell death, no net charge should be transferred from the electrode into tissue, i.e., charge balance principle should be kept when stimulation occurs [11]. Fig. 2 shows a common charge-balanced biphasic stimulating pulse format. Key parameters of this stimulating pulse include frequency, amplitude and width. The first parameter affects smoothness of nerve contractions and needs to be adjusted to prevent nerve fatigue while the latter two parameters affect strength of contraction by altering the charge injected. To achieve good stimulating results, all these parameters should be strictly controlled.

For the stimulator described in this work, an important consideration is to realize accurate and flexible control on pulse parameters with simple circuits and low power consumption. Therefore, several design techniques are adopted to make the circuit flexible, simple and low-power.

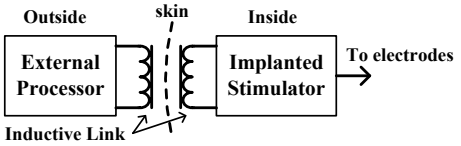

Figure 1. Common structure for wireless electrical stimulation system

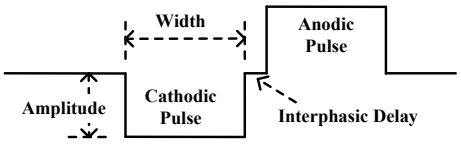

Figure 2. Biphasic current stimulating pulse waveform

II. Overview of the Implantable Stimulator

The block diagram of the proposed implantable stimulator is shown in Fig. 3. It can be divided into two groups of circuits: front-end and back-end circuits. The front-end circuit consists of full-wave rectifier, voltage regulator, power-on reset generator, envelope detector, waveform calibration, and clock and data recovery. It provides power for the whole chip, extracts clock and instruction trains from the wireless signal and generates a reset signal at power-on. The back-end circuit consists of digital control logic, digital-to-analog converter, voltage controlled current source, and switch array. It is the primary part of the stimulator that generates stimulating pulses to drive the electrode array.

To realize accurate and flexible control on pulse parameters with simple circuits and low power consumption, the proposed stimulator has following features:

(1) A simple but effective ASK modulation scheme with delicate encoding method is adopted.

(2) A versatile power generating structure provides the whole chip with voltage as low as possible to minimize power consumption.

(3) A voltage controlled current source with a dual-voltage -source scheme guarantees accurate stimulating current output and high stimulating efficiency.

*Resrach supported by the National Natural Science Foundation of China (No. 61006022).

Songping Mai is with Lab. of Integrated Circuits and Systems Design, Graduate School at Shenzhen, Tsinghua University, Shenzhen 518055, China (phone: +86-755-26036420; fax: +86-755-26036352; e-mail: mai.songping@sz.tsinghua.edu.cn).

Zhijun Wang, Chun Zhang and Zhihua Wang are with Institute of Microelectronics, Tsinghua University, Beijing 100084, China (email: zhihua@tsinghua.edu.cn).

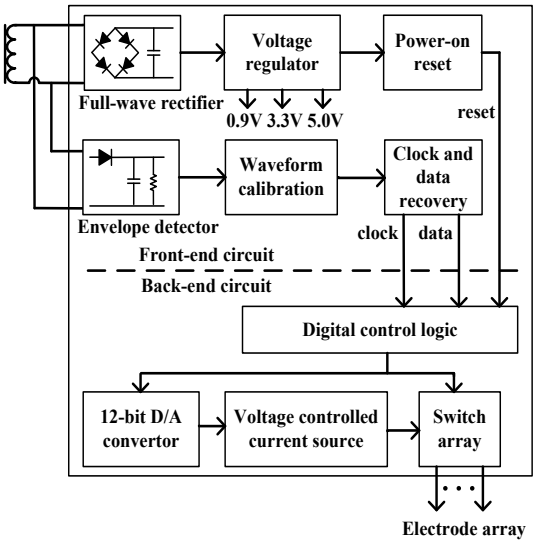

Figure 3. Block diagram of the implantable stimulator

Frame	S	M	A	W	EL1	EL2	C
Bit	1	1	12	6	5	5	1

Figure 4. Format of wireless instruction data frame

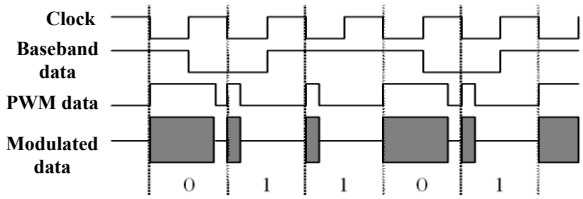

Figure 5. Modulation process and waveform

(4) A flexible switch array is used to realize quick switching and keep charge balance among stimulating electrodes.

III. Wireless Transmission Protocol and Modulation/Demodulation Scheme

The wireless inductive link is to establish control over as well as to provide power to the implantable stimulator, thus a data transmission protocol to program the stimulating pulses and a modulation scheme which ensures a sufficient power supply should be addressed.

A. Transmission protocol

Stimulating instruction data are transferred in frames, whose format is shown in Fig. 4. Each frame is 31-bit long, composed of all necessary information to generate a pulse, including pulse amplitude ('A'), pulse width ('W') and serial numbers of two selected electrodes ('EL1' and 'EL2'). The 'S' segment is the start (synchronized) indication bit which is a constant one since zeros are filled between frames, while the 'C' segment is the parity bit that ends the frame. The 'M' defines two stimulating modes: common-ground and paired. In common-ground mode, the ground electrode is pre-defined, while the firing electrode is specified in 'EL1', and 'EL2' is left empty; In paired mode, the firing electrode and the ground electrode are specified in 'EL1' and 'EL2', respectively.

The implantable stimulator accordingly generates pulse immediately after it receives an instruction frame, so the stimulating pulse frequency is controlled by the data frame rate. At a data rate of 500Kbps, taking a 31-bit frame and at least 1-bit interval into account, the maximum frame (or stimulating pulse) frequency is 15,625 Hz.

B. Modulation scheme

The base-band data are first encoded in a pulse-width-modulation (PWM) manner, and then modulated in a carrier of 13.56MHz using amplitude shift keying (ASK). The carrier frequency of 5MHz~15MHz has been proven safe by commercial cochlear implants, so we chose 13.56MHz, a mature RFID frequency, as the carrier frequency. It can simplify the RF circuit design, achieve proper inductive coupling efficiency, and reduce electromagnetic absorption of the tissue at low frequency [12]. The relationship among clock, baseband data, PWM data and ASK modulated signal is shown in Fig. 5. The PWM data which have duty cycles of 3/4 and 1/4 are used to represent baseband data "0" and "1", respectively. They are further modulated using ASK and then transmitted from the external circuit into the implanted stimulator. As the PWM signal is self-timing, the implanted stimulator can easily extract both data and clock from the wireless signal with very simple circuit.

It should be noted that, even at the interval between two instruction frames, the implanted stimulator is still working and consuming power. To provide more power for the stimulator, the datum "0" which fills between frames has larger duty cycle (3/4) than the datum "1" (1/4).

C. Demodulation circuit

The demodulation circuit and its node waveform are shown as Fig. 6. First, envelope of the modulated signal on the implantable secondary coil is extracted (Node 'A'). Then a Schmitt trigger is used to regulate the envelope waveform and form the PWM data (Node 'B'). The PWM data contain periodic pulses (with either 3/4 or 1/4 duty cycles) whose rising edges are strictly periodically. These can be further regulated by a monoflop to generate periodic pulses with uniform 1/2 duty cycles (Node 'Clock Out') which can be used as the global clock of the implantable circuit. Finally the baseband data are derived by sampling the PWM data using this global clock (Node 'Data Out').

D. Power recovery

The power recovery circuit shown in Fig. 7 is used to generate supply voltage to power the whole implantable circuit. The carrier wave first goes through a full-wave rectifier, generating a DC voltage (approximately 5~10V). This voltage depends heavily on coupling condition of the two coils and is not very stable. It then goes into a high-voltage bandgap and produces a coarse reference voltage (1.2V). With 5~10V as input voltage and 1.2V as reference voltage, two series low-dropout regulators generate two voltages (5.0V and 3.3V). The previous one (5.0V) is used as high stimulating voltage, while the latter (3.3V) is used as low stimulating voltage and supply voltage for the digital control logic, the voltage controlled current source and the switch

array. Finally, a low-voltage bandgap uses the 3.3V voltage input to generate a high-precision 0.9V voltage, which is used as the DAC reference voltage.

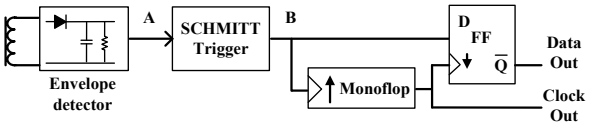

Figure 6(a). Demodulation circuit

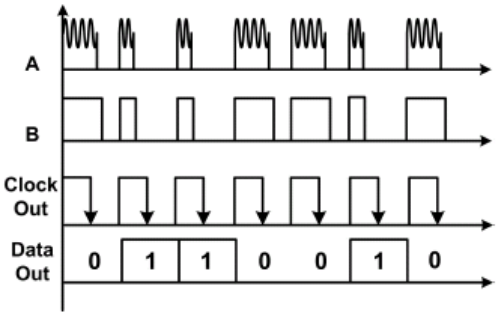

Figure 6(b). Demodulation process and waveform

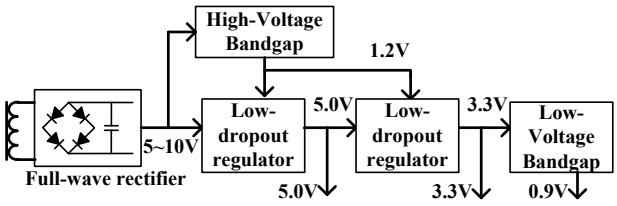

Figure 7. Power recovery circuit

IV. Stimulating Output Stage

To achieve charge balance, a voltage controlled biphasic current stimulating method (corresponding pulse waveform shown in Fig. 2) is adopted. The stimulating circuit, which consists of a D/A convertor (DAC), a voltage controlled current source (VCCS), a switch array and a digital controller, is shown as the back-end circuit in Fig. 3. In the following, we will focus on the low-power, programmable pulse generating circuit design.

A. Voltage controlled current source

The voltage controlled current source (VCCS), shown as Fig. 8(a), is composed of an OPA and a feedback transistor *M*. Due to the negative feedback mechanism of the OPA, the voltage on the resistor *R* equals to the output voltage of the DAC, which is totally determined by the DAC input, or the wirelessly transmitted amplitude value. Therefore, the stimulating current can be expressed as followed:

$$Iout=V_{DAC}/R$$

Once the DAC input is settled and the tissue load falls into reasonable range, the stimulating current will keep constant.

B. Dual-voltage-source scheme

The equivalent circuit of the stimulating output stage is shown in Fig. 8(b), where I_{out} and R_T respectively denote the stimulating current and the tissue load between two selected electrodes. The output energy efficiency of the stimulating circuit can be defined as

$$\eta = \frac{I_{out}^2 \cdot R_T}{Vdd \cdot I_{out}} = \frac{I_{out} \cdot R_T}{Vdd}$$

Obviously, the output efficiency changes with the stimulating current in proportion. When the current is small, the voltage drop on R_T keeps low and most of the power is dissipated on R_V (equivalent total resistor of the transistor *M* and the resistor *R*), resulting in large energy waste.

To reduce this kind of energy waste, a dual-voltage-source scheme is adopted. As shown in Fig. 9, there are two voltage sources, *VH* and *VL*, of which one is selected to drive the electrodes according to the digital input. Once the digital input is larger than a given threshold, the high voltage source *VH* is selected; otherwise the low voltage source *VL* is used. By cutting down the voltage drop on R_V when the stimulating current is small, the output efficiency is raised and the power consumption is reduced.

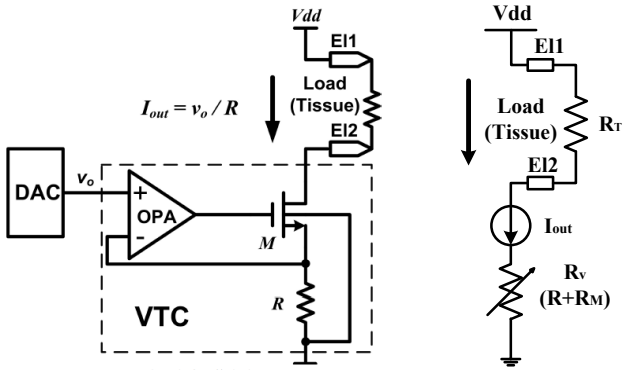

Figure 8. (a) Structure of stimulating circuit with controllable current source (b) Equivalent circuit

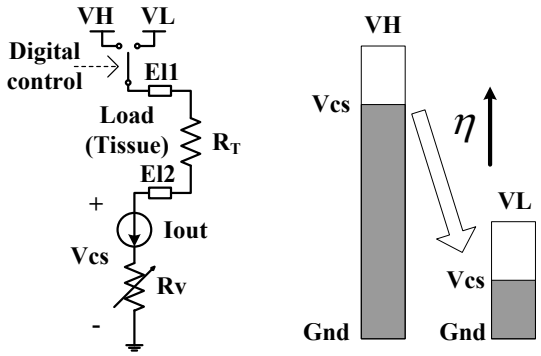

Figure 9. Dual-voltage-source scheme

C. Switch array

To realize quick switching between stimulating electrodes, a switch control array is proposed and partly shown in Fig. 10. The voltage sources *VH* and *VL* respectively represent the high voltage and low voltage power supplies, and the current source is the above mentioned VCCS. There are four connection switches (transmission gate pairs SVHx, SVLx, SCx and Sx) for every electrode, via which the electrode can be connected with the high voltage source, the low voltage source, the current source, or shorted with other electrodes.

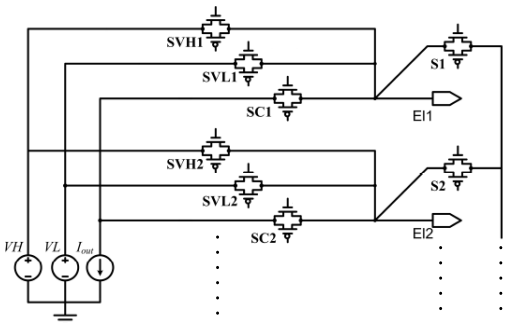

Figure 10. Structure of switch control array

When an electrode is inactive or at interphasic delay, only the corresponding switch Sx is on and all other switches SVHx, SVLx and SCx are off. At such condition, all electrodes are shorted together to guarantee the charge balance. When a high-voltage anodic pulse occurs between two electrodes, e.g. El1 and El2, the switches S1 and S2 will turn off, and SVH1 and SC2 will turn on, which generates constant current flowing from El1 to El2. Other conditions may be deduced by analogy.

D. Digital control logic

The control logic is a simple digital circuit, whose clock and data inputs come from the demodulation module. Once detecting a start bit from the data input stream, it begins to extract the pulse amplitude, pulse width and the selected electrode numbers, and then performs the parity check. If the data frame is correct, the pulse amplitude data will be sent to the DAC, and the pulse width and the selected electrode numbers will be used to control the switch array.

V. Chip Implementation and Measurement Result

The proposed stimulator chip is fabricated in Chartered 0.35-μm Embedded EEPROM high voltage CMOS process. Its micrograph is presented in Fig. 11 and total silicon size including input/output pads is 2.50mm x 2.75mm. Strict measurement is carried out as followed.

A. Measurement setup

As shown in Fig. 12, the measurement system is built up by imitating a wireless stimulator system which consists of two circuit boards, an implanted board and an external board.

As the only chip on the implanted board, the proposed stimulator chip is bonded with an inductive coil and several capacitors and resistors. The external board mainly contains a microcontroller, a 13.56MHz RFID reader chip and an inductive coil. Both two inductive coils have an identical diameter of 33mm.

When measurement is performed, the two inductive coils are placed at a coaxial spacing of approximate 2.5mm and tuned to resonate at 13.56MHz. The microcontroller generates stimulating instruction trains, and then the RFID reader chip sends these trains to the implanted board via the coupled coils. The transmission protocol and modulation scheme are coherent with those described in Section III. To ensure power supply to the implanted board, 10% ASK modulation depth is adopted, and transmission power varies at several tens of milliwatts depending on working conditions.

At the stimulating output stage, as the maximum DAC output voltage is 0.9V (equal to the DAC supply voltage), to achieve a maximum stimulating current of 2mA, an off-chip 450Ω resistor is used as the resistor R in Fig. 8. The tissue load between any two selected electrodes depends on the metal contact area of the electrode-tissue interface, and can be usually modelled as a resistor of several kilo-ohms. In this work, a 2KΩ resistor is used to model the tissue load between two selected electrodes (i.e. the resistor R_T in Fig. 8).

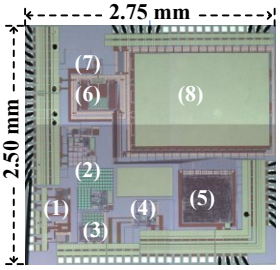

(1) Rectifier
(2) Bandgap
(3) LDOs
(4) Data & clock recovery
(5) Control logic
(6) DAC
(7) VCCS
(8) Switch array

Figure 11. Die micrograph

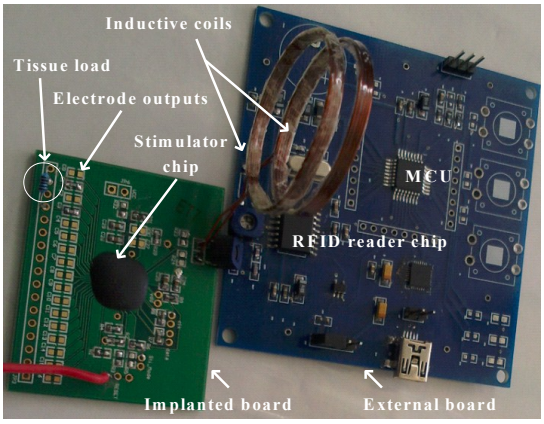

Figure 12. Measurement system

B. Measurement results

The chip measurement begins with a series of tests of electrical characteristics, covering all LDO and bandgap voltage outputs. After confirming that all output voltages are at expected levels, we then focus on functional and power tests, among which data demodulation, stimulating output and overall chip power consumption are most concerned.

(1) Data demodulation

Fig. 13 shows waveform of a series of demodulated PWM data. It can be compared with the waveform of Node 'B' in Fig. 6. Although there are glitches at each level transition and the duty cycles are not very stable, data "1" and "0" which have respectively approximate 1/4 and 3/4 duty cycles are still distinguished from each other and can be easily identified by digital logic.

(2) Stimulating output

According to demodulated stimulating instructions, the stimulating output stage generates stimulating pulses and exerts them on two selected electrode outputs. Fig. 14 shows a

group of stimulating pulses with different amplitude and width observed between two selected electrode outputs. Each stimulating output is a biphasic pulse. As described in Section IV, they are ideally charge-balanced and suitable for neural stimulation.

More detailed measurement results of the stimulating output are shown in Table 1.

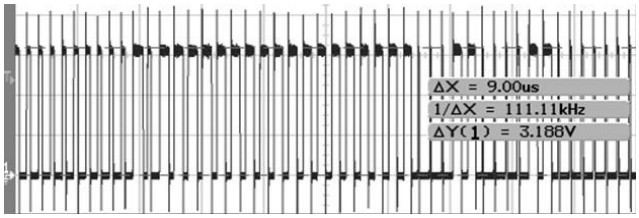

Figure 13. Demodulated PWM data waveform

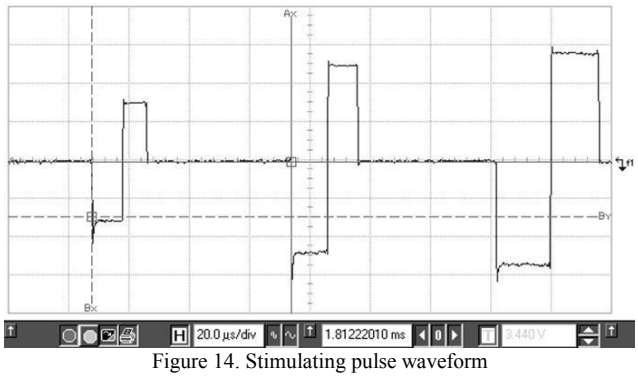

Figure 14. Stimulating pulse waveform

TABLE 1. PARAMETERS OF THE STIMULATING OUTPUT

Carrier freq./Max data rate	13.56MHz/500Kbps
Max stimulating rate*/Channels	15Kpps/16
Stimulating pulse type	Dual-phase/constant current
Pulse amplitude/steps	0~2mA/4096
Pulse width/steps	4~130us/64

*Note: The output stage doesn't support parallel stimulation, so the maximum stimulating rate is for only one channel.

(3) Overall chip power consumption

The inductive link is adjusted to keep the induced peak voltage of the implanted coil higher than 8V, guaranteeing sufficient power supply to the implanted circuit. Then the external circuit generates and sends certain stimulating instructions, and the induced average RMS current of the implanted coil is measured at the below conditions:

- No tissue load. The stimulator chip keeps generating stimulating pulses of arbitrary amplitude and width according to received instructions with all electrode output floating.
- Typical stimulation with 2KΩ load. The stimulator chip keeps generating stimulating pulses of 0mA, 1mA or 2mA amplitude according to received instructions with two selected electrodes connected by a 2KΩ resistor as the tissue load.

Table 2 lists the measurement result. It can be derived that the chip itself consumes less than 1mA current, exclusive of the stimulating current dissipated on the tissue load. And even taking the stimulating current into account, the total current consumption of the chip is also less than 3mA at maximum stimulating output condition. As power consumption depends heavily on working condition, different types of stimulators have no comparability on this issue. But for neural stimulation applications, the proposed stimulator chip is very low power and competent.

TABLE 2. CURRENT CONSUMPTION OF THE STIMULATOR CHIP

Pulse amp. / Tissue load	Arbitrary	0mA	1mA	2mA
No load	905uA	---	---	---
2KΩ load	---	1080uA	1956uA	2765uA

VI. CONCLUSION

The design and implementation of an implantable stimulator chip is presented. By adopting a series of design techniques like PWM embedded ASK modulation, versatile power supply, dual-voltage-source stimulation, flexible switch array, and so on, the chip achieves very accurate and flexible control on stimulating pulse parameters, including frequency, amplitude and width, with simple circuits and low power consumption. Featuring high stimulating rate, large current driving capacity and low power consumption, the proposed chip is suitable for various neural stimulation applications, like spinal cord stimulator or cochlear implant.

REFERENCES

[1] P. M. Zoll, "Resuscitation of the heart in ventricular standstill by external electric stimulation," New Eng. J. Med., vol. 247, no. 20, pp. 768–771, 1952.

[2] B. Smith, P. H. Peckham, M. W. Keith, and D. D. Roscoe, "An externally powered, multichannel, implantable stimulator for versatile control of paralyzed muscle," IEEE Trans. Biomed. Eng., vol. BME-34, no. 7, pp. 499–508, 1987.

[3] B. Linderoth and R. D. Forman, "Physiology of spinal cord stimulation: Review and update," Neuromodulation, vol. 2, no. 3, pp. 150–164, 1999.

[4] P. Loizou, "Introduction to cochlear implants," IEEE Eng. Med. Biol. Mag, vol. 18, no. 1, pp. 32–42, 1999.

[5] R. Sarpeshkar, "Ultra Low Power Bioelectronics: Fundamentals, Biomedical Applications, and Bio-Inspired Systems," Cambridge, U.K.: Cambridge Univ. Press, 2010.

[6] R. A. Normann, E. M. Maynard, P. J. Rousche, and D. J. Warren, "A neural interface for a cortical vision prosthesis," Vision Res, vol. 39, no. 15, pp. 2577–2587, 1999.

[7] L. Xiao, A. Demosthenous, and N. Donaldson, "An Integrated Stimulator With DC-Isolation and Fine Current Control for Implanted Nerve Tripoles," IEEE Journal of Solid-State Circuits, vol. 46 (7), pp. 1701–1714, Jul 2011.

[8] S. K. Kelly, and J. L. Wyatt, "A Power-Efficient Neural Tissue Stimulator With Energy Recovery," IEEE Transactions on Biomedical Circuits and Systems, vol. 5 (1), pp. 20–29, Feb 2011.

[9] S. K. Arfin, M. A. Long, M. S. Fee, and R. Sarpeshkar, "Wireless Neural Stimulation in Freely Behaving Small Animals," Journal of Neurophysiology, vol 102 (1), pp. 598–605, Jul 2009.

[10] L. Jongwoo, R. Hyo-Gyuem, D. Kipke, and M. Flynn, "A 64 Channel programmable closed-loop deep brain stimulator with 8 channel neural amplifier and logarithmic ADC," 2008 IEEE Symposium on VLSI Circuits, pp. 76–77, Jun 2008.

[11] Stuart F. Cogan, "Neural Stimulation and Recording Electrodes," Annual Review of Biomedical Engineering, vol. 10, pp. 275-309, Aug 2008.

[12] W. T. Jonines, "Frequency-Dependent Absorption of Electromagnetic Energy in Biological Tissue," IEEE Transactions on Biomedical Engineering, Vol.BME-31, pp. 17-20, Jan. 1984.